Citation: DING Xiaoqi, LIU Xin, QI Zhuangzhuang, ZHANG Wei, LIU Sihong. Reservoir space characterization of vuggy carbonate reservoirs with multiple scales:a case study of Ma 5-7 interval, Middle Ordovician Majiagou Formation, Daniudi area, Ordos Basin[J], Petroleum Geology & Experiment, 2021 (4): 689-696.

The English version here is roughly translated and has not been reviewed or edited. Please contact us if you need a finely translated and edited version.

Reservoir space characterization of vuggy carbonate reservoirs with multiple scales:a case study of Ma 5-7 interval, Middle Ordovician Majiagou Formation, Daniudi area, Ordos Basin

DING Xiaoqi[1], LIU Xin[1], QI Zhuangzhuang[1], ZHANG Wei[2], LIU Sihong[2]

1. Energy College, Chengdu University of Technology, Chengdu 610059, Sichuan;
2. North China Company, SINOPEC, Zhengzhou 450006, Henan

Abstract: The reservoir space of carbonate rocks is of multiple scales and genesis mechanisms, and it is difficult to accurately demonstrate the reservoir space as well as physical properties. Millimeter-, micro-and nano-scale reservoir spaces were all developed in the Ma 5-7 interval (the 7 th sub-member of the 5th member) of the Ordovician Majiagou Formation in Daniudi area, Ordos Basin. In order to study the storage space and physical properties, the storage space was characterized in layers at multiple scales, and combined with the approach of logging curves, a calculation model was established for the description of pores and caves. Several conclusions were made as follow. (1) For carbonate rock reservoirs with storage space of multiple scales, we can accurately describe their storage space by the means of core rubbing for dissolved pores (> 1 mm), case thin section for intercrystalline pores (> 2 μm), and argon ion polishing-scanning electron microscope for submicron and nano pores (< 2 μm). (2) On the basis of multi-scale reservoir space characterization, the acoustic porosity and neutron-density porosity can be constrained, and the corresponding intercrystalline pore porosity calculation model and dissolved pore porosity calculation model can be established, which have higher calculation accuracy.

Keywords: vuggy reservoir; reservoir space; carbonate rock; Majiagou Formation; Daniudi gasfield; Ordos Basin; Ordos Basin

Along with the exploration and development, it has been discovered that deep carbonate rocks still contain superior oil and gas reserves and act as the priority of further hydrocarbon exploration [1-2]. For example, the development of macroscopic dissolved caves could be observed in the carbonate rocks with the burial depth of over 8 000 m in the Well TS1, in the Tarim Basin [3]. Due to unstable composition, multi-scale storage space (e.g. pores, caves and fractures) could be developed in carbonate rocks. The study on their storage space and physical properties by individual method is limited and inaccurate. LI Yilin et al. [4] used nanometer and micrometer CT, automatic mineral identification system (QEMSCAN), MAPS image junction technology and environment scanning electric microscope (ESEM) and other new unconventional testing technologies to characterize the storage space of tight Gaotaizi Oil Layer in the Qijia Area in macroscopic and microscopic scales. LI et al. [5]applied CT scanning technology to study on the fractures and caves of carbonate rocks and on different pore types by image extraction, dissection and calculation. WANG Lu et al. [6] utilized cast thin sections, SEM, high-pressure mercury injection experiment and CT scanning method to study and analyze on reservoir samples from the Deng-4 Member in the Gaoshiti-Moxi Area, Sichuan Basin and to quantitatively characterize pore texture features of vuggy carbonate reservoirs. CORBETT et al. [7]studied on pore types and textures of microbial reservoirs by the combination of outcrop photographs, image analysis, CT description and computer simulation in order to deal with multi-scale storage space characterization of microbial rocks.

The Ma 5-7 interval in Ordovician Majiagou Formation, Ordos Basin is a newly-discovered gas layer in recent years. This interval is a suite of tight micritic dolostone intercalated with two or three powdered dolostone layers with gypsum nodules; each single layer is roughly 2 m thick. The moldic pores of gypsum nodules were formed by fresh water leaching in the Caledonian. Meanwhile, dolomite crystals with gypsum nodules are coarser than those of micritic dolomite.

Received: 2020-09-01
Supported by: National Oil & Gas Major Project (2017ZX05005-001-010); SINOPEC Department of Science and Technology Key Project (P20043-2); Higher Education Talent Training Quality and Teaching Reform Key Project (JG182017)
First author: DING Xiaoqi (1981–), male, PhD, associate professor, engaged in the research on carbonate reservoir geology. E-mail: xiaoqiding@qq.com.

© 2021 China Academic Journals (CD Edition) Electronic Publishing House Co., Ltd.

In the powdered dolostone, the size of intercrystalline pores is in the range of 20–30 μm; while in the micritic dolostone, generally smaller than 10 μm. The size of gypsum moldic pores are ranges from several millimeters to 1–2 cm. They are round and egg-shaped, and distributed uniformly in the powdered dolostone. This suite of the powdered dolostone with moldic pores has good physical properties and high gas content. Because the entire gypsum moldic pores are difficult to be included in cast thin sections, the percentage of the moldic pores in the thin sections is hard to estimate accurately. At the same time, a large amount of moldic pores lead to difficult coring of small columns so that the measured porosity is often the sum of the matrix porosity and a part of cast porosity of the dolostone. It is difficult to accurately demonstrate the reality of reservoir physical properties. In the calculation of reservoir physical property parameters by logging data, common acoustic data could not reflect actual reservoir physical properties precisely due to the occurrence of isolated moldic pores. All of them cause the difficulty of gas content assessment and reserve calculation on Ma 5-7 interval.

In this article, by the application of the JMicroVision Software, the intercrystalline pores of cast thin sections from the Ma 5-7 interval of the Daniudi, Ordos Basin were extracted; the size distribution of pore diameter and thin section porosity of micrometer-scale intercrystalline pores were analyzed; the coring samples were photographed and made rubbing; and the moldic pores in core rubbing were extracted to measure the pore diameter size and percentage of moldic pores in millimeter and centimeter scales. After the argon ion polishing, the samples were observed by the SEM to study on the size and thin section porosity of intercrystalline micropores with the size of over tens of nanometers. By the constrains of the thin section porosity of intercrystalline pores (including nanometer-scale ones), the calculation model was constructed based on acoustic matrix porosity. By the constrains of total thin section porosity, the calculation model was constructed based on total neutron-density porosity. Finally, this study method was discussed on the aspects of its applicability and limitations in the characterization of multi-scale storage space of carbonate rocks.

1 Regional geologic characteristics

In Ordovician, the Ordos Area belonged to a part of the North China Platform with epicontinental deposits [8]. The Daniudi Gas Field is situated in northern Yishan Slope with the acreage of 2 000 km^2 (Fig. 1). Previous exploration focused on mainly Upper Paleozoic tight sandstone gas [9]. In recent years, mainly weathering crust gas reservoirs [10-11] (mainly Ma 5-1+2 intervals) and dolostone gas reservoirs [12] (mainly Ma 5-5 interval) have been discovered in the exploration on Lower Paleozoic Ordovician. Along with continuous exploration, good dolostone reservoirs have been encountered in the drilling of Ma 5-7 interval; industrial gas flows have been produced in several wells; and they have superior gas exploration potential.

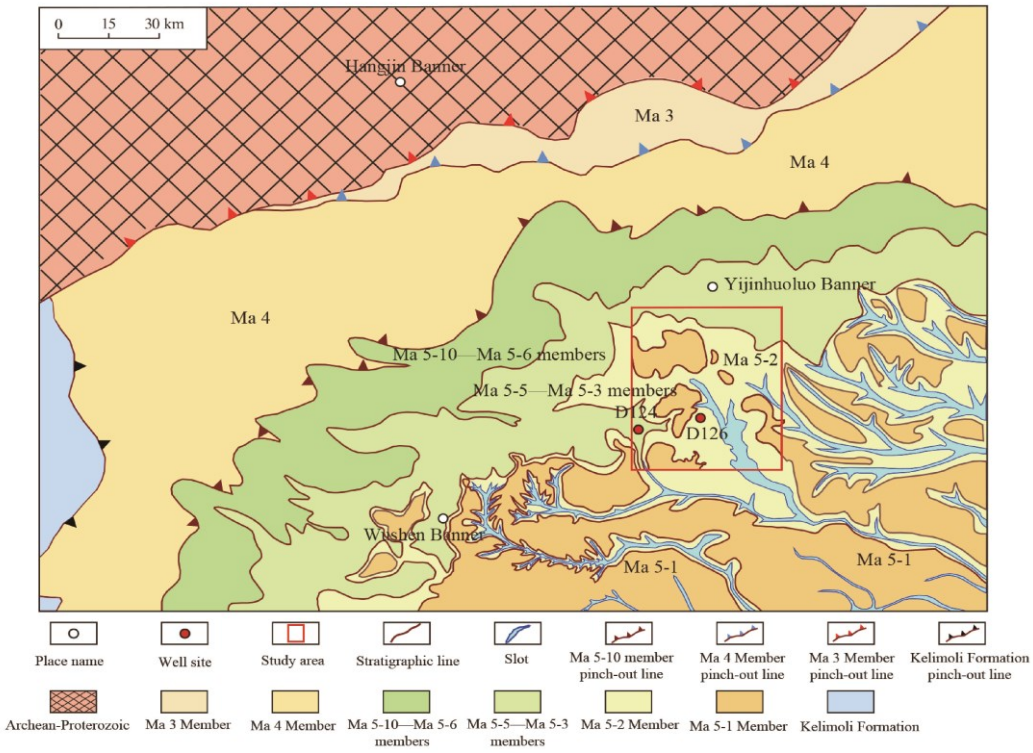

Fig. 1 Location of Daniudigas field and paleogeologic map of pre-Carboniferous, Ordos Basin

© 2021 China Academic Journals (CD Edition) Electronic Publishing House Co., Ltd.

Lower Ordovician Yeli and Liangjiashan formations are absent in the Ordos Basin, and Middle Ordovician Majiagou Formation has unconformable contact with underlying Cambrian [7]. According to lithologic assemblage characteristics, the Majiagou Formation in this basin could be divided into six members from bottom to top. Ma 1, 3 and 5 members were formed in the regression stage with mainly the dolostone intercalated with gypsum and halite with variable thickness and relatively high clay content. Ma 2, 4 and 6 members were formed in the transgression stage with mainly the limestone with variable dolostone content. Due to small paleo-continent outcrops, they contain roughly no clay with limited debris supplies [13]. From bottom to top, Ma 5 Member could be subdivided into ten intervals. Ma 5-9, 5-7, 5-5 and 5-1+2 intervals contain mainly thick-layered and massive limestone and dolostone with few gypsum nodules, representing short-term transgression in the regression background. However, Ma 5-10, 5-8, 5-6 and 5-3+4 contain mainly laminated, thin-layered and medium-layered clayey dolostone and gypsum-rich dolostone with gypsum and halite interlayers locally, representing a large-scale regression. In this article, main horizon discussed is the Ma 5-7 interval that has stable distribution in the study area, 13–20 m thick, as a suite of the dolostone with penecontemporaneous genesis.

Due to the Caledonian Movement in late stage of Early Paleozoic, overlying strata of the Ma 5 Interval were leached by atmospheric fresh water to form karst reservoirs. In the study area, Ma 6 and part of Ma 5 intervals were eroded into a hiatus. The outcrops below the unconformity were mainly Ma 5-2 and 5-3 intervals (Fig. 1). In the Caledonian, the depth of fresh water leaching was large [10-11] and the erosion depth was down to Ma 5-7 interval due to high palaeogeomorphic position of the Daniudi. The gypsum nodules were dissolved by fresh water to form moldic pores (Figs. 2 and 3). Therefore, the powdered crystalline dolostone with moldic pores has good physical properties and acts as main gas layers in the Ma 5-7 interval. However, the micritic crystalline dolostone in the Ma 5-7 interval has no intercrystalline pores and insignificant late-stage dissolution by fresh water due to its non-plane anhedral crystals. $\frac{1}{4}$ The reservoir type of the Ma 5-7 interval has similar characteristics as that of Ma 5-1 and 5-4-1 intervals [14].

2 Storage space

In the powdered-crystalline dolostone with moldic pores in the Ma 5-7 interval, the size of dolomite crystals is usually found in the range of 50–100 μm with mainly planar subhedral crystals. The storage space includes intercrystalline pores (micrometer-scale) and intracrystalline pores (nanometer-scale) of the dolomite and moldic pores (millimeter-centimeter-scale) formed by the dissolution of gypsum nodules (Figs. 3 and 4) without significant fractures. The intercrystalline pores occur mostly in the area of the development of euhedral dolomite crystals, while the development of moldic pores is at random but in relatively stable horizons.

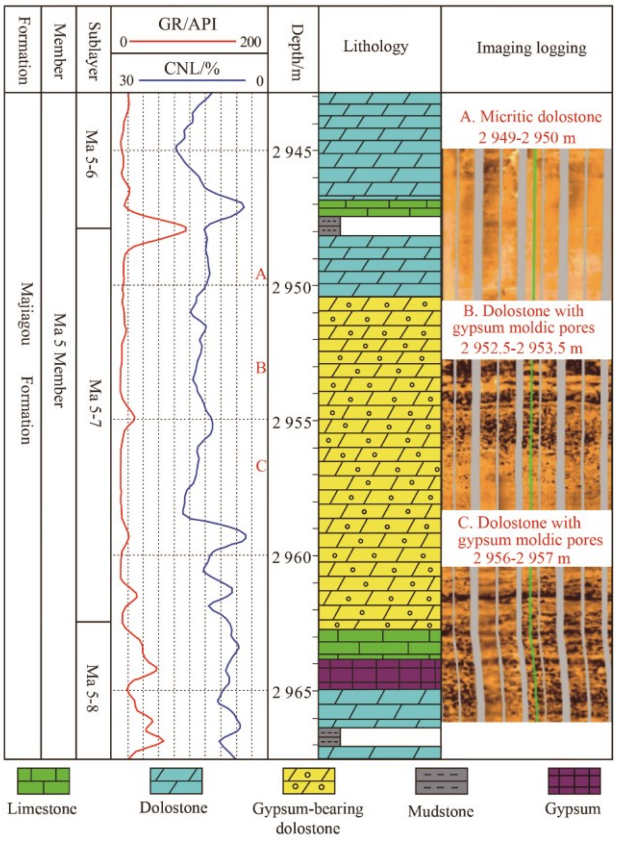

Fig. 2 Stratigraphic column of Ma 5-7 interval of Middle Ordovician Majiagou Formation, well Da 126, Daniudi gas field, Ordos Basin

2.1 Moldic pore characterization

According to core images (Fig. 3), the moldic pores were extracted by the core rubbing method. Because only over 1 mm moldic pores could be extracted generally by this method so that the resolution is 1 mm. After the core rubbing, the moldic pores were extracted by the JMicroVision Software to analyze on pore diameter distribution and thin section porosity of moldic pores. Fig. 3 shows that (1) the moldic pores are distributed extensively but with uneven size distribution; (2) the diameter of moldic pores is mostly in the range of 2–8 mm, the number of moldic pores with the diameter larger than 1 cm is rare but has large acreage percentage; (3) the thin section porosity of moldic pores is in the range of 4%–7% and 5.87% on average.

2.2 Intercrystalline pores

The pores in cast thin sections were extracted, and the size distribution and the thin section porosity of intercrystalline pores were calculated by the JMicroVision Software (Fig. 4). Fig. 4 displayed that: (1) the minimum pore diameter extracted by this method is 2 μm; and with respect to the

© 2021 China Academic Journals (CD Edition) Electronic Publishing House Co., Ltd.

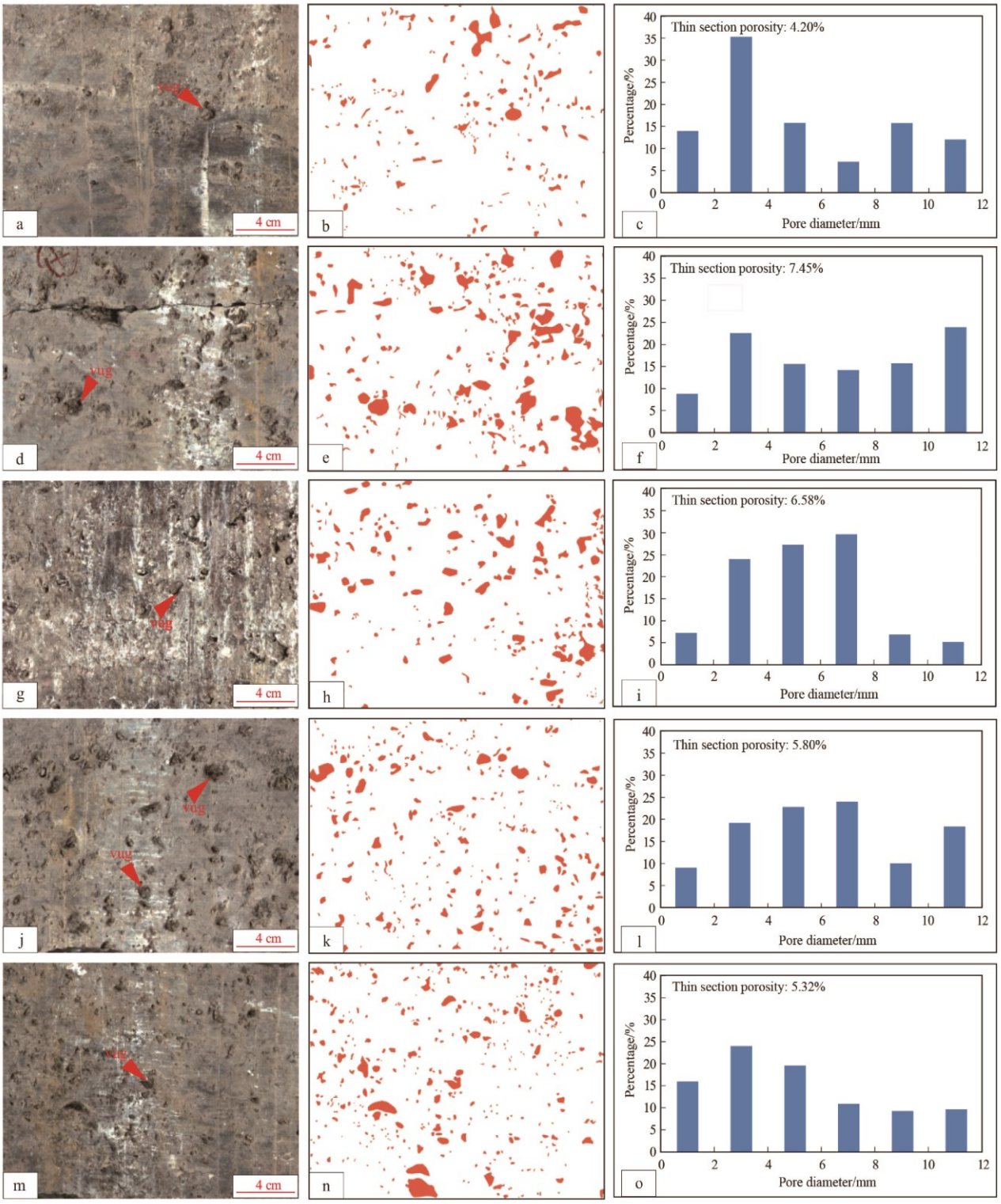

Fig. 3 Core photographs, rubbing moldic pore and vuggy radii distribution of Ma 5-7 interval of Middle Ordovician Majiagou Formation, well Da 124, Daniudi gas field, Ordos Basin

a. powdered crystalline dolostone, 3 150.15 m; b. pore distribution diagram of Fig. a; c. moldic pore distribution histogram of Fig. a; d. powdered crystalline dolostone, 3 152.8 m; e. pore distribution diagram of Fig. d; f. moldic pore distribution histogram of Fig. d; g. powdered crystalline dolostone, 3 153.1m; h. pore distribution diagram of Fig. g; i. moldic pore distribution histogram of Fig. g; j. powdered crystalline dolostone, 3 153.28 m; k. pore distribution diagram of Fig. j; l. moldic pore distribution histogram of Fig. j; m. powdered crystalline dolostone, 3 153.9 m, plain light; n. pore distribution diagram of Fig. m; o. moldic pore distribution histogram of Fig. m.

© 2021 China Academic Journals (CD Edition) Electronic Publishing House Co., Ltd.

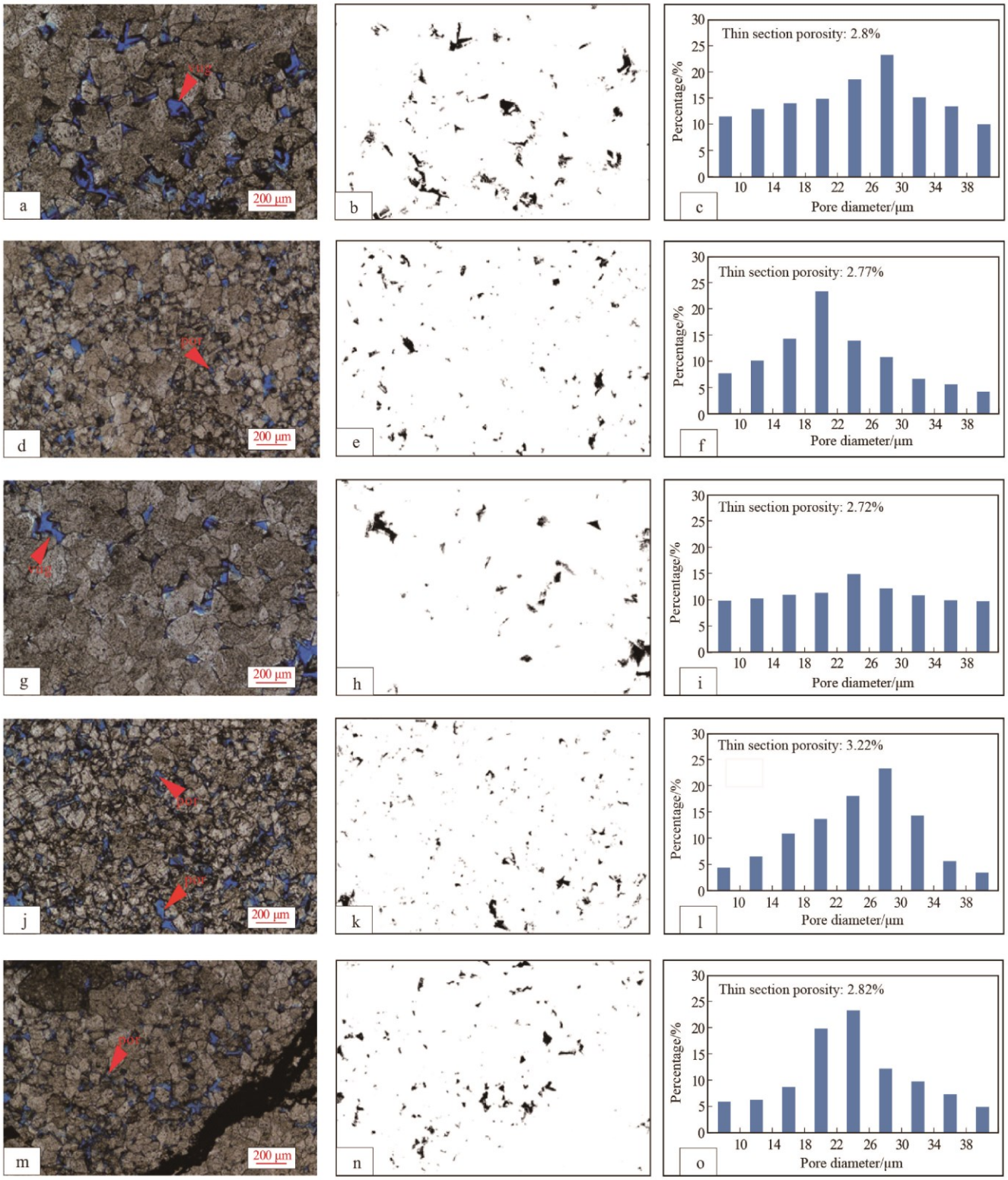

Fig. 4 Photomicrographs of crystalline dolomites, distribution of pores and pore radii of Ma 5-7 interval of Middle Ordovician Majiagou Formation, well Da 124, Daniudi gas field, Ordos Basin

a. powdered crystalline dolostone, 3 150.15 m; plainlight; b. pore distribution diagram of Fig. a; c. intercrystalline pore distribution histogram of Fig. a; d. powdered crystalline dolostone, 3 152.80m; plain light; e. pore distribution diagram of Fig. d; f. intercrystalline pore distribution histogram of Fig. d; g. powdered crystalline dolostone, 3 153.10m, plainlight; h. pore distribution diagram of Fig. g; i. intercrystalline pore distribution histogram of Fig. g; j. powdered crystalline dolostone, 3 153.28 m, plainlight; k. pore distribution diagram of Fig. j; l. intercrystalline pore distribution histogram of Fig. j; m. powdered crystalline dolostone, 3 153.90m, plain light; n. pore distribution diagram of Fig. m; o. intercrystalline pore distribution histogram of Fig. m.

© 2021 China Academic Journals (CD Edition) Electronic Publishing House Co., Ltd.

intercrystalline pores smaller than 2 μm, they could not be extracted by the limitations of cast image resolution; (2) intercrystalline pore diameter is mainly distributed in the range of over 6μm and concentrated in the range of 20-30μm; (3) the thin section porosity is in the range of 2%–4%, intercrystalline pores are in uniform and normal distribution.

2.3 Nanometer-submicrometer intracrystalline-intercrystalline pores

With respect to nanometer-submicrometer pores smaller than 2μm, their genesis might be related with the bonding surfaces of crystals or lattice defect in the crystal growth (Fig. 5). In this article, the argon ion polishing-SEM was applied in the study. According to the statistics on nanometer-submicrometer pores (smaller than 2μm) and intercrystalline pores (larger than 2μm) in five samples, it was discovered that the porosity of nanometer-submicrometer pores was 0.9% on average. Therefore, the porosity of nanometer-submicrometer pores was low and could be estimated by the Equation (1) (Fig. 6a).

$$\varphi_{In} = 0.27\varphi_{Iin} + 0.14 \quad (1)$$

In which, φ_{In}-the porosity of nanometer-submicrometer pores; φ_{Iin}-the porosity of intercrystalline pores.

Therefore, the total reservoir porosity is the sum of moldic porosity, intercrystalline porosity and nanometer- submicrometer porosity.

3 Reservoir porosity characterization

3.1 Total porosity characterization

The neutron could reflect hydrogen content. The hydrogen content is the highest in the water but low in natural gas, so the neutron porosity in gas layers would become lower to generate "excavation effect" [15]. The dolostone in the Ma 5-7 interval is pure with low clay content and nearly without inter-clay micropores or textual water. Therefore, the neutron porosity could not be calibrated by the mud. The Ma 5-7 interval has tight lithology and regular borehole wall so that its density is reliable. When there is the natural gas in the reservoirs, the density would get lower and the porosity calculated by the density would be larger. Therefore, the total porosity calculated by the neutron and density could diminish the influence of natural gas to a large extent. In comparison with the total porosity characterized by the layering and multiple scales (Figs. 6b and 7), both of them have good correlation. The total porosity could be calculated by the following two equations (2) and (3).

$$\varphi_t = 0.02 \times \sqrt{(\varphi_\rho^2 + \varphi_{Cnl}^2)/2} + 8.05 \quad (2)$$

$$\varphi_\rho = (\rho_m - \rho)/(\rho_m - \rho_f) \quad (3)$$

In which, φ_t-total porosity, %; φ_ρ-density porosity, %; φ_{Cnl}-compensated neutron porosity, %; ρ_m-dolostone matrix density, 2.87 g/cm^3; ρ_f-fluid density, 1.0 g/cm^3; ρ-rock density, g/cm^3;

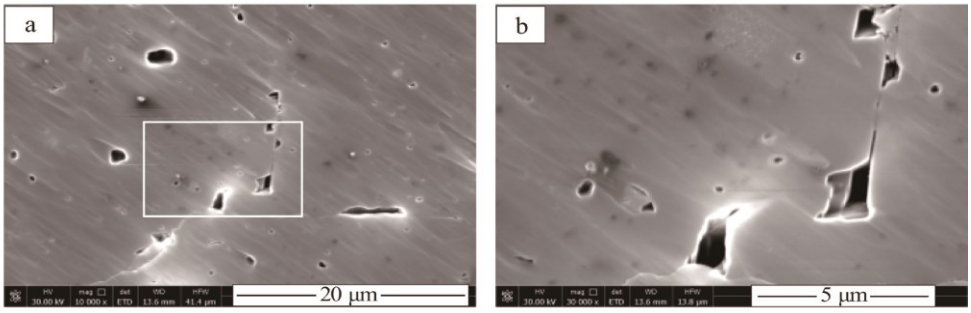

Fig. 5 SEM photomicrographs of nanometer- and sub- micrometer-pores in dolomites, Ma 5-7 interval of Middle Ordovician Majiagou Formation, Daniudi gas field, Ordos Basin

(b) is an enlargement of the white box in (a) (well da 124, 3 152.47 m).

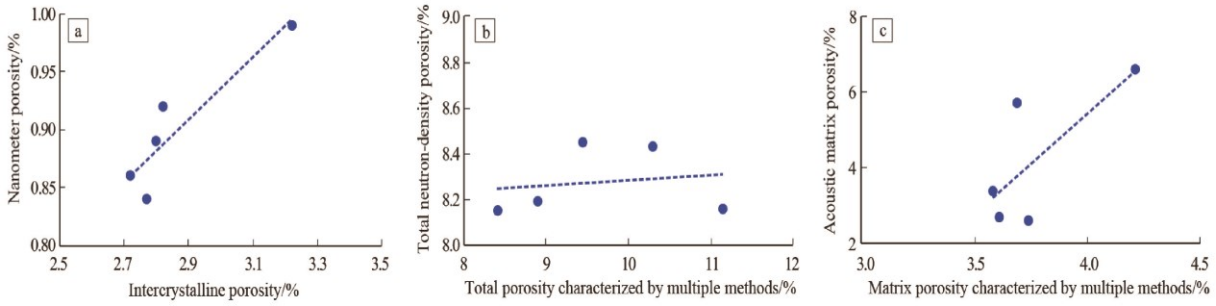

Fig. 6 Crossplots of dolomite porosities of Ma 5-7 interval of Middle Ordovician Majiagou Formation, Daniudi gas field, Ordos Basin

© 2021 China Academic Journals (CD Edition) Electronic Publishing House Co., Ltd.

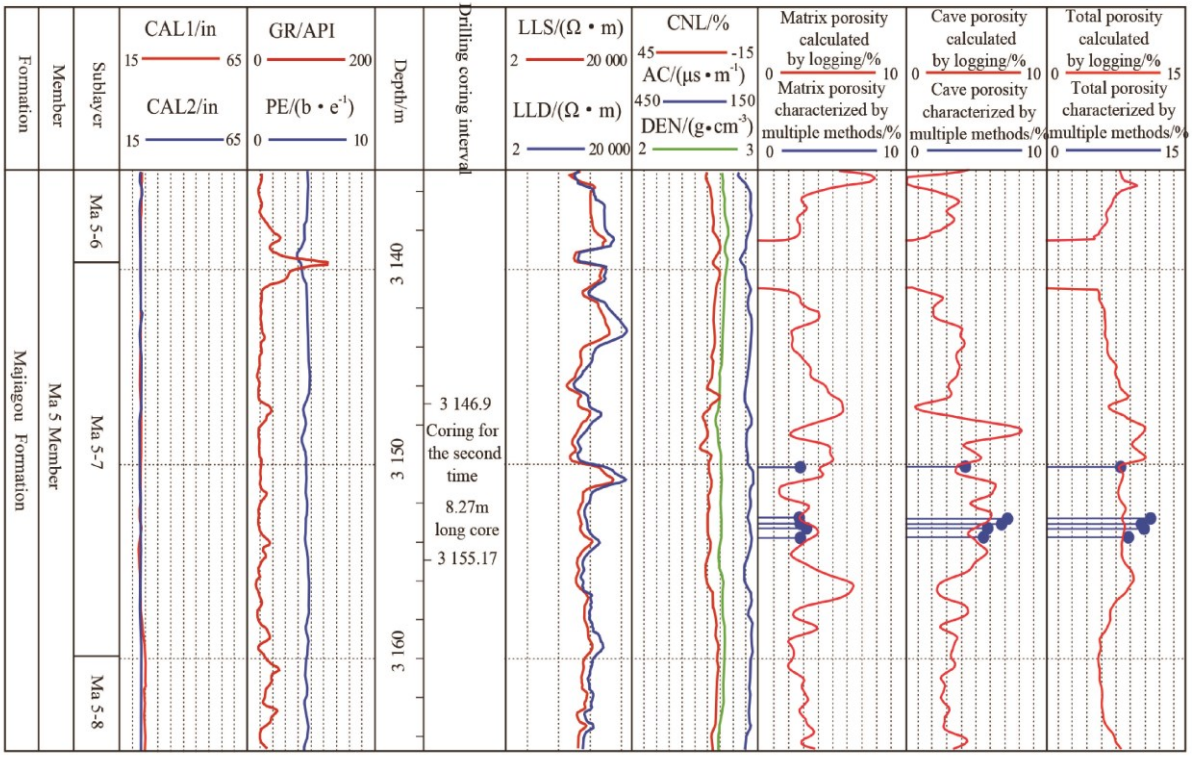

Fig. 7 Comparison of interpreted porosity of well logging and measured porosity of well Da 124, Daniudi gas field, Ordos Basin

3.2 Matrix porosity characterization

The acoustic transmission velocity is different in diverse media. However, the acoustic logging is measured as the head P wave velocity along the shortest transmission time. In general, it is considered that the acoustic travel time is not affected by the caves and high-angle fractures but only affected by the matrix and intergranular pores [15]. The acoustic wave reflects the information about connecting porosity and the matrix. Isolated caves could not be reflected in acoustic logging curves. Therefore, the porosity calculated by acoustic logging often act as the matrix porosity. Based on the regression of characterized matrix porosity (Fig. 6c), the calculation equation of the acoustic (matrix) porosity in the dolostone is shown as the following equation (4).

$$\varphi_{ac}=5.26(AC-AC_{ma})/(AC_{fld}-AC_{ma})-15.59 \quad (4)$$

In which, φ_{ac}-acoustic porosity, %;A C-acoustic travel time, μm/s; AC_{ma}-dolostone matrix acoustic travel time, 145 μm/s; AC_{fld}-fluid matrix acoustic travel time, 620 μm/s.

In terms of the comparison of the porosity calculated by acoustic curves and intercrystalline and intracrystalline porosities characterized by multiple methods (Fig. 7), both of them have good correlation. Therefore, the dolostone matrix porosity could be calculated by acoustic curves.

3.3 Moldic porosity characterization

The moldic porosity is obtained after the total porosity calculated by the neutron and density is deducted by the matrix porosity calculated by acoustic travel time. Fig. 7 shows that the moldic porosity is in the range of 4%–6% and 5.1% on average, which is in correspondence with the value (5.87% on average) characterized by five sample rubbings.

4 Discussions

4.1 Feasibility and limitations of characterization on layering and multi-scale storage space

The moldic pore diameter in the Ma 5-7 interval is in the range of 1–20mm with average thin section porosity of 5.87%; the intercrystalline pore diameter, 20–30μm with average thin section porosity of 2.87% and roughly 0.9% submicrometer-nanometer pores lower than 2μm. The analysis on moldic intercrystalline pores in thin sections shows that, although the distribution of dolostone intercrystalline pores is relatively uniform, they still have certain heterogeneities and could not be amplified too much. Otherwise, the work load could multiply and it could generate the differences arouse by the heterogeneities (worse viewing area representativeness) [7]. In this article, the cast thin sections are amplified for 100 times and the minimum identifiable pore diameter is 1–2μm. However, a large amount of intracrystalline-intercrystalline nanometer-submicrometer pores smaller than 2μm could be observed in the argon ion polishing SEM. In other words, the intercrystalline pores calculated by the JMicroVision Software are only macroscopic (>2μm). In

© 2021 China Academic Journals (CD Edition) Electronic Publishing House Co., Ltd.

combination with argon ion polishing SEM, intercrystalline (intracrystalline) porosity could be approximated and represented by the calibration coefficient calculated by the regression method.

In the process of core rubbing, the minimum identifiable pore diameter is generally over 1mm. Therefore, the moldic pores with the pore diameter higher than 1mm could be characterized accurately if the enough samples are available. Because the coring length is generally several meters in the intervals of interest, the core rubbing length is not constrained and could be accomplished by both core slicing and core circular scanning, both of which have no essential differences but the moldic pores are seen with better clarity by previous method. At present, the cores from most of oil fields are scanned digitally to provide the conveniences for the study on large-scale pores and caves. After the rubbing of plane core maps, the slices are put into the JMicroVision Software to set the scale and extract pores and caves to study on the distribution of pore diameter and their percentages. With respect to the core rubbing, it is required generally that dissolved caves are smaller than a half of core diameter; while for larger-scale caves, their percentage could only be determined by the outcrops.

Therefore, multi-layer characterization on the dolostone storage space in the Ma 5-7 interval (millimeter-scale core rubbing, micrometer-scale cast thin sections and submicrometer-nanometer-scale aragon ion polishing SEM) could describe multi-scale storage space of this dolostone suite accurately.

4.2 Feasibility of unconnected moldic porosity calculated by tri-porosity logging

In general, it is considered that the acoustic travel time could only reflect the connecting porosity and not isolated dissolved cave porosity. Therefore, the acoustic porosity is generally lower than total porosity calculated by the neutron and density. The acoustic porosity of the Ma 5-7 interval is approximate to intercrystalline porosity (including nanometer porosity). Fig. 7 shows that the absolute error of the acoustic porosity and characterized intercrystalline porosity is 1.31%.

The total porosity is calculated by the combination of the neutron and the density, which could diminish natural gas excavation effect and higher density porosity generated by the natural gas to a large extent. The neutron-density porosity calculation equation has no realistic meanings only when the total porosity is calibrated by layering characterization to generated the value that has realistic meanings. Isolated moldic porosity equals to the value deducted by the intercrystalline porosity calculated by acoustic travel time. This calculated moldic porosity is approximate to the value characterized by core rubbing with 0.88% absolute error, which could meet the requirements. The calculation of unconnected porosity is significant for the quantitative identification on carbonate reservoir types.

5 Conclusions

(1) With respect to the carbonate reservoirs with multi-scale storage space, the characterization on the storage space is uncertain by single method that could not characterize the size, distribution, quantity and spatial distribution of the storage space accurately and objectively. The multi-scale storage space of carbonate rocks could be characterized accurately by the combination of the studies on dissolved caves extracted by core rubbing (> 1 mm), intercrystalline pores extracted by cast thin sections (> 2 μm), submicrometer-nanometer pores (< 2 μm) in argon ion polishing SEM.

(2) Based on the characterization on multi-scale storage space, it could constrain acoustic porosity and neutron-density porosity and construct the calculation models of corresponding intercrystalline porosity and dissolved cave porosity. These models have higher calculation accuracy.

(3) Representative samples from the target intervals are required in the characterization on layering and multi-scale storage space of carbonate rocks. In other words, medium-scale heterogeneity is relatively weak (with uniform distribution of intercrystalline pores and moldic pores). If the heterogeneity is too strong with the development of fractures, it would be difficult to constrain acoustic porosity and total neutron-density porosity.

References

[1]WANG Dapeng,BAI Guoping,XU Yan,et al.Characteristics and hydrocarbon distribution of the Paleozoic giant marine carbonate rock oil-gas fields in the world[J].Journal of Palaeogeography,2016,18(1):80-92.

[2]MA Yongsheng,CAI Xunyu,ZHAO Peirong.The research status and advances in porosity evolution and diagenesis of deep carbonate reservoir[J].Earth Science Frontiers,2011,18(4):181-192.

[3]YUN Lu,ZHAI Xiaoxian.Discussion on characteristics of the Cambrian reservoirs and hydrocarbon accumulation in well Tashen-1,Tarim Basin[J].Oil & Gas Geology,2008,29(6):726-732.

[4]LI Yilin,ZHANG Yunfeng,YIN Shuli,et al.Characterization of the pore space in tight sandstone reservoirs from macroscopic and microscopic perspectives:a case study of Gaotaizi reservoir in Qijia area,the Songliao Basin[J].Oil & Gas Geology,2016,37(6):915-922.

[5] LI Binhui,TAN Xuequn,WANG Fuyong,et al.Fracture and vug characterization and carbonate rock type automatic classification using X-ray CT images[J].Journal of Petroleum Science and Engineering,2017,153:88-96.

[6]WANG Lu,YANG Shenglai,PENG Xian,et al.Pore structure characteristics and storage-seepage capability of multi-type reservoirs in fracture-cavity carbonate gas reservoirs:a case study of Deng-4 member in Gaoshiti-Moxi area,Sichuan Basin[J].Journal of Jilin University (Earth Science Edition),2019,49(4):947-958.

[7] CORBETT P,HAYASHI F Y,ALVES M S,et al.Microbial carbo-nates:a sampling and measurement challenge for petrophysics addressed by capturing the bioarchitectural components[M].London:Geological Society,2015.

[8]FENG Zengzhao.Lithofacies paleogeography of Early Paleozoic of North China platform[M].Beijing:Geological Publishing House,1990.

[9]DING Xiaoqi,ZHANG Shaonan,ZHOU Wen,et al.Characteristics and genesis of the Upper Paleozoic tight sandstone reservoirs in the northern Ordos Basin[J].Oil & Gas Geology,2007,28(4):491-496.

[10]JIA Huichong,DING Xiaoqi.Characteristics of dolomite karst reservoirs in the M51+2 Member of Majiagou Formation,Daniudi gas field,Ordos Basin,China[J].Journal of Chengdu University of Technology(Science &

© 2021 China Academic Journals (CD Edition) Electronic Publishing House Co., Ltd.

Technology Edition),2016,43(4):415-422.
[11]DING Xiaoqi,ZHANG Shaonan,PAN Huaixiao,et al.Development patterns of collapse-type karst reservoirs in the Ordovician of Daniudi gasfield,Ordos Basin[J].Oil & Gas Geology,2016,37(2):210-217.
[12]LIU Mei,DING Xiaoqi,WAN Youli,et al.Characteristics and distribution of Ordovician weathering crust reservoirs in Daniudi gasfield,Ordos Basin[J].Marine Origin Petroleum Geology,2014,19(1):35-42.
[13]WANG Linlin,FU Yun,FANG Shijie.Elemental geochemical characteristics and geological significance of Majiagou Formation,eastern Ordos Basin[J].Petroleum Geology & Experiment,2018,40(4):519-525.
[14]HE Jiang,FENG Chunqiang,MA Lan,et al.Diagenesis and diagenetic facies of crust-weathered ancient karst carbonate reservoirs[J].Petroleum Geology & Experiment,2015,37(1):8-16.
[15] LUCIA F J.Carbonate reservoir characterization[M].New York: Springer,2007.

(Translated by [译者])

CNKI

© 2021 China Academic Journals (CD Edition) Electronic Publishing House Co., Ltd.